acta physica slovaca vol. 47 No. 3/4, 233 – 242 June 1997

SIMULTANEOUS MULTIMODE OPTICAL PARAMETRIC OSCILLATION IN A TRIPLY RESONANT CAVITY[1]

M. Marte, H. Ritsch[2]
Institut für Theoretische Physik, Universität Innsbruck, Technikerstr. 25, A-6020 Innsbruck, Austria

L. Lugiato
Dipartimento di Fisica, Università degli Studi di Milano, Via Celoria 16, Milano 20133, Italy

C. Fabre
Laboratoire Kastler Brossel, Université Pierre et Marie Curie, 75252 PARIS cedex 05 France

Received 30 April 1997, accepted 12 May 1997

We investigate the triply resonant optical parametric oscillator using a spherical mirror cavity and a finite-sized pump. We show that, depending on the size of the pump and the cavity geometry, a cross-coupling between different pairs of oscillating cavity modes occurs. This leads to a modification of the oscillation threshold and allows simultaneous oscillation of several mode pairs with fixed relative phases. Several distinct stable solutions with different thresholds can be found and simultaneous degenerate and nondegenerate operation is predicted. This implies the appearance of transverse optical field patterns above threshold.

1. Introduction

Nowadays the optical parametric oscillator (OPO) has become a device with a broad range of applications (cf. the recent contributions to special issues on second order non-linear processes [1]). A quantum description usually starts with a model Hamiltonian involving a (quantized) pump mode and a single or a pair of modes for the signal and idler fields, which are coupled by some effective nonlinear coupling constant. All the other modes in the cavity are usually neglected, as they are assumed either to be far off resonance or dynamically uncoupled. In general this assumption is not valid and

[1] Presented at the **Fifth Central-European Workshop on Quantum Optics**, Prague, Czech Republic, April 25 - 28, 1997

[2] E-mail address: Helmut.Ritsch@uibk.ac.at

0323-0465/97

higher order transverse modes play an important role in the dynamics, forming optical patterns above threshold [2] and modifying the nonclassical photon correlations below threshold [3]. In addition, for a resonator with nonplanar mirrors, a finite-sized pump yields an extra nonlinear coupling between different signal and idler mode pairs. This introduces a strikingly different physical behaviour of the system and leads to new and interesting phenomena such as combined oscillation of various modes above threshold with fixed relative phase or multistability between such solutions.

2. Model

We consider a cavity with spherical mirrors and a *thin* nonlinear χ^2-crystal inside. The cavity is coherently pumped at a frequency ω_p from the outside and the mirrors are assumed highly reflective at the pump frequency as well as around the signal ω_s and idler ω_i frequencies, with $\omega_s + \omega_i = \omega_p$, i.e. we consider the triply resonant case of an OPO with a common cavity for all fields. Neglecting the influence from the thin crystal we use an expansion of all fields in Laguerre-Gaussian modes [4]

$$\begin{aligned} U_{np\ell}(r,\phi,z) &= e^{-ik_{np\ell}z}\, u_{np\ell}(r,\phi,z) \quad \text{for} \quad p=0,1,2,\ldots;\ \ell=0,\pm1,\pm2,\ldots \\ u_{np\ell}(r,\phi,z) &= \sqrt{\frac{2p!}{\pi(p+|\ell|)!}}\,\frac{1}{w(z)}\left[\frac{\sqrt{2}r}{w(z)}\right]^{|\ell|} L_p^{|\ell|}\left(\left[\frac{\sqrt{2}r}{w(z)}\right]^2\right)\times \\ &\quad \exp\left\{-i\,\frac{k_{np\ell}\,r^2}{2q(z)} + i(2p+|\ell|+1)\arctan\left(\frac{z}{z_0}\right)\right\} e^{i\ell\phi}, \end{aligned} \tag{1}$$

where the functions $L_p^{|\ell|}$ are the Laguerre polynomials. As always the wavevectors $k_{np\ell}(z) = \omega_{np\ell}\, n(z)/c$ that allow stable selfreproducing oscillatory solutions have to be determined from the boundary conditions (including the refractive index $n(z)$ of the crystal). Here $w(z)$ denotes the waist function $w^2(z) = w_0^2(1+(z/z_0)^2)$ with $w_0^2 = 2z_0/k_{np\ell}$ the minimal waist and z_0 denoting the Rayleigh length. $q(z) = z + iz_0$ is defined as a 'complex curvature'. In this basis our model Hamiltonian reads:

$$H = H_0 + H_P + H_C + H_R \tag{2}$$

$$H_0 = \sum_{\{j_p\}} \hbar\omega_{j_p} a_{j_p}^{+} a_{j_p} + \sum_{j\in\{j_s,j_i\}} \hbar\bar{\omega}_j a_j^{+} a_j \tag{3}$$

$$H_P = i\hbar \sum_{\{j_p\}} (Q_{j_p} e^{-i\omega_p t} a_{j_p}^{+} - e^{i\omega_p t} a_{j_p} Q_{j_p}^{*}) \tag{4}$$

$$H_C = i\hbar g \sum_{\{j_s,j_i,j_p\}} \chi_{\{j_s,j_i\}}^{j_p} (a_{j_p} a_{j_s}^{+} a_{j_i}^{+} - a_{j_p}^{+} a_{j_s} a_{j_i}) \tag{5}$$

$$H_R = \sum_{j\in\{j_s,j_i,j_p\}} (a_j^{+}\Gamma_j + a_j\Gamma_j^{+});, \tag{6}$$

with $a_{j_p}, a_{j_s}, a_{j_i}$ being the mode annihilation operators for the pump, signal and idler modes, respectively, and Γ_i being independent bath operators describing the damping of

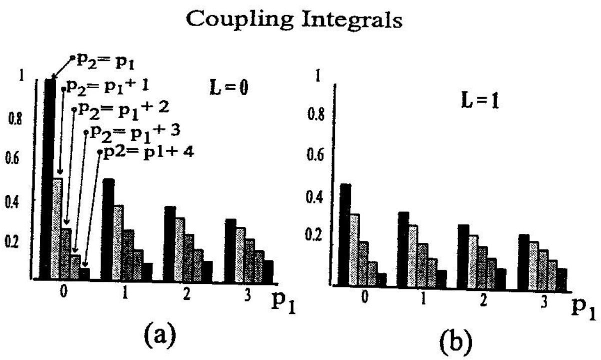

Fig. 1. Transverse part $\chi_\perp$ of the nonlinear coupling integrals for a TEM_{00} pump mode ($L = |\ell|$).

the various modes including diffraction losses and absorption by the crystal. $\{j_p, j_s, j_i\}$ are combined indices for the mode quantum numbers $j_\nu = \{n_\nu, p_\nu, \ell_\nu\}, \nu \in \{p, s, i\}$ for each mode. The frequencies ω_j for the set of *relevant* modes $\{j_p, j_s, j_i\}$ depend on the cavity and crystal geometry, for which we have three cases in mind, namely a quasiplanar, quasiconfocal or quasispherical cavity. The parameters

$$Q_{j_p} = \int_{F_{mirror}} d^2x\, U_{j_p}^{*}(\vec{x})\, E_p(\vec{x}) \tag{7}$$

describe the linear coupling of the various pump modes to the external pump field $E_p(\vec{x})$; in the case of pumping at the fundamental mode we have $Q_{j_p} = \epsilon\, \delta_{(p_p,0)}\, \delta_{(l_p,0)}$.

For a short crystal we approximate the nonlinear coupling integral $\chi_{j_s,j_i}^{j_p}$ [5] by

$$\chi_{j_s,j_i}^{j_p} = \chi_{L_c}^{z} \int_{F_{crystal}} dr d\phi\, U_{j_p}(r,\phi,0)\, U_{j_s}^{*}(r,\phi,0)\, U_{j_i}^{*}(r,\phi,0)\,. \tag{8}$$

The factor χ^z in front of the integral reflects the longitudinal phase mismatch (on-axis), which for the moment we will assume to be slowly varying for the considered modes (thin medium). A more detailed and systematic treatment will be given elsewhere [6].

From symmetry considerations it follows that the angular part of these integrals vanishes except for $\ell_p = \ell_s + \ell_i$. Thus we get $\ell_s = -\ell_i$ for a pure TEM_{00} mode in the pump field. Assuming a crystal cross-section much larger than the mode functions, the transverse (r,ϕ) integral can be evaluated analytically for almost degenerate signal and idler frequencies with beam waists $w_p = w_0(k = k_{j_p})$ and $w_s = w_i$, yielding

$$\chi_{\perp\,(n,p_1,\ell),(n,p_2,-\ell)}^{(n,0,0)} = \sqrt{\frac{8}{\pi}}\,\frac{w_p}{2w_p^2 + w_{i,s}^2}\,\frac{1}{2^{p_1+p_2+|\ell|}}\,\frac{(p_1+p_2+|\ell|)!}{\sqrt{p_1!\,p_2!\,(p_1+|\ell|)!(p_2+|\ell|)!}}\,. \tag{9}$$

The lowest few of these integrals giving the coupling of the TEM_{00} mode to modes with ℓ=0 and $\ell = \pm 1$, are graphically visualized in Fig. 1a and 1b.

The most striking difference to the ordinary OPO-treatment appears, if one looks at the radial indices p. The nonlinear coupling imposes little restriction on possible combinations of radial modes, and a coupling of the $p_p = 0$ mode to different signal/idler pairs $\{p_s, p_i\}$ occurs. One might say that a photon in the pump mode can now be split either into a degenerate pair of the same radial index $p_s = p_i$ or into a nondegenerate pair $p_s \neq p_i$. (Actually one has a superposition of all these possibilities.) This is related to the radial confinement of the pump field, which leads to a transverse momentum uncertainty, weakening the transverse pair correlation. Note for comparison that in the case of a plane wave pump, the orthogonality of the modes implies $p_i = p_s$ and no such cross-coupling occurs [3].

3. Semiclassical analysis of the case with two OPO modes

In order to work out the main physical implications of this mode coupling process, let us now consider the simplest nontrivial case where such a phenomenon can be studied. For this we assume most couplings χ to be small or the corresponding mode detunings large, so that besides one pump mode, only two more modes, a_1 and a_2, effectively take part in the downconversion process. For example we take only the largest 3 couplings of Fig. 1a into account. Although a bit unrealistic, this gives some understanding of the underlying physical mechanisms. For simplicity we label the three relevant modes simply by 0, 1, 2, with index 0 belonging to the pump mode.

Starting from the Hamiltonian truncated to three modes, neglecting quantum noise and transforming the rapid optical oscillations away, we end up with the following equations for the slowly varying mode amplitudes α_i

$$\begin{aligned} \dot{\alpha_0} &= (-\gamma_0 + i\Delta_0)\,\alpha_0 - \chi_1\,\alpha_1^2 - \chi_2\,\alpha_2^2 - \chi_{12}\,\alpha_1\alpha_2 + E_p \\ \dot{\alpha_1} &= (-\gamma_1 + i\Delta_1)\,\alpha_1 + 2\chi_1\,\alpha_0\alpha_1^* + \chi_{12}\,\alpha_0\alpha_2^* \\ \dot{\alpha_2} &= (-\gamma_2 + i\Delta_2)\,\alpha_2 + 2\chi_2\,\alpha_0\alpha_2^* + \chi_{12}\,\alpha_0\alpha_1^* \,. \end{aligned} \tag{10}$$

Here γ_i is the decay rate of the i-th mode and the detunings Δ_i are defined as $\Delta_0 = \omega_0 - \omega_p$, $\Delta_1 = \omega_1 - \omega_s$ and $\Delta_2 = \omega_2 - \omega_i$.

For simplicity we have assumed all nonlinear coupling constants χ_i to be real. Note that the limiting case $\chi_{12} = 0$ corresponds to the usual degenerate OPO case (actually two degenerate OPOs), while the case $\chi_1 = \chi_2 = 0$ gives the nondegenerate OPO. In our model with a finite sized pump field, both processes occur simultaneously.

In the special case $\chi_{12} = 2\sqrt{\chi_1\chi_2}$ it is possible to introduce a linear combination $b = \sqrt{\chi_1/(\chi_1+\chi_2)}\,a_1 + \sqrt{\chi_2/(\chi_1+\chi_2)}\,a_2$ as a new mode operator with proper commutation relations leading to the simple form $H_C = i\hbar\,\sqrt{\chi_1+\chi_2}\,(a_0^\dagger b^2 - h.c.)$ for the nonlinear Hamiltonian. Hence it is possible to interpret the interaction of the 3 modes including degenerate and nondegenerate downconversion processes and cross-coupling as a single rescaled degenerate OPO. In general, however, we have to consider several simultaneous nonlinear processes.[3]

3.1. Steady states and threshold conditions

Fortunately, in this model limited to 3 modes in total, the steady state amplitudes of the fields and the corresponding oscillation thresholds can be found analytically. As in the standard case for a weak pump field, up to a first threshold only the pump mode oscillates, while the semiclassical amplitudes of all other modes are zero

$$\alpha_0^0 = E_p;\ \alpha_1^0 = \alpha_2^0 = 0\,. \tag{11}$$

Above this first threshold, for *nonzero* χ_{12} there exist nontrivial steady state solutions with definite relative phases. Choosing the pump field amplitude E_p real and positive, the possible solutions fullfill: $\alpha_i^0 = r_i\,e^{i\varphi_i}$ with $\varphi_i = m\frac{\pi}{2}$ and $m \in \{-1,0,1,2\}$. As the most striking difference to the usual NDOPO, where the amplitudes do not have well-defined steady state phases, but only the sum phase is fixed, we find that simultaneous oscillation of both modes with well-defined steady phases occurs. Note that even very weak cross-coupling leads to locking of the phases. Above a second threshold, there are further nontrivial steady state with *opposite* sign in α_1 and α_2;

Introducing the scaled quantities $h_1 = \sqrt{(\gamma_2/\gamma_1)}(\chi_1/\chi_{12})$, $h_2 = (\sqrt{\gamma_1/\gamma_2})(\chi_2/\chi_{12})$, and $h_{12}^2 = 1 + (h_1 - h_2)^2$ we find explicitly:

a) solutions with same sign:

For pump fields E_p above the first threshold

$$E_{T_1} = \frac{\gamma_0\sqrt{\gamma_1\,\gamma_2}}{\chi_{12}}\,\frac{1}{h_1 + h_2 + h_{12}} > 0\,, \tag{12}$$

the following $\pm$ pair of solutions appears

$$\begin{aligned} \alpha_0^0 &= \frac{E_{T_1}}{\gamma_0} \\ \alpha_1^0 &= \pm\sqrt{\sqrt{\frac{\gamma_2}{\gamma_1}}\frac{E_p - E_{T_1}}{\chi_{12}h_{12}\,[1 + 2h_2(h_{12} - h_1 + h_2)]}}, \quad \alpha_2^0 = (\alpha_1^0)_{\substack{\gamma_1\leftrightarrow\gamma_2 \\ h_1\leftrightarrow h_2}}\,. \end{aligned} \tag{13}$$

b) solutions with opposite sign:

The threshold for this type of solution occurs at $|E_{T_2}| > E_{T_1}$ with

$$E_{T_2} = \frac{\gamma_0\sqrt{\gamma_1\,\gamma_2}}{\chi_{12}}\,\frac{1}{h_1 + h_2 - h_{12}}\,, \tag{14}$$

---

[3] Note that in the rather restrictive case of only one pump mode $j_p = j_{p_0}$ involved, with $\chi^{j_{p_0}}_{j_s,j_i}$ being real and symmetric and complete degeneracy (including equal cavity decay rates!) of all signal/idler modes, one can transform to a basis where we get an uncoupled set of DOPO'S as treated in Ref. [3], with modified basis functions. As these conditions are rather restrictive, we will not pursue this approach further and stay with the natural uncoupled cavity basis.

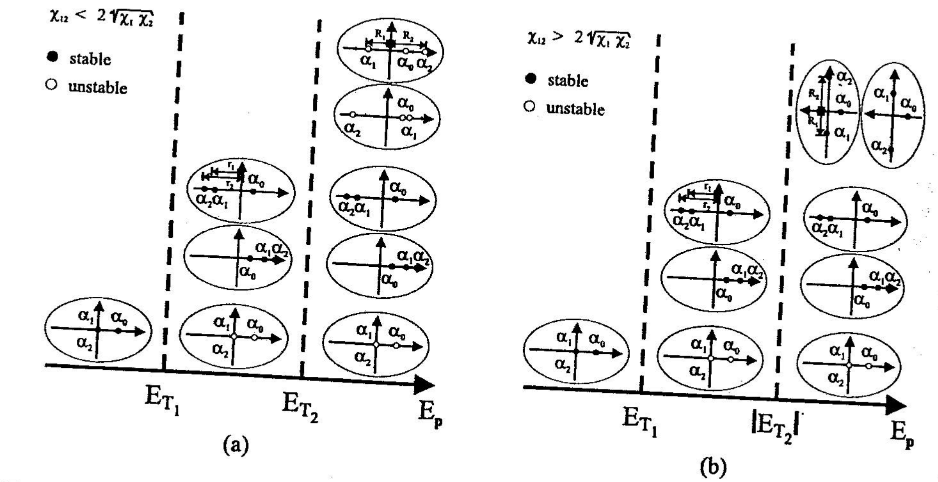

Fig. 2. Type and stability of stationary solutions.

and we have to distinguish the two cases:

i) For *weak cross-coupling* ($\chi_{12} < 2\sqrt{\chi_1\,\chi_2}$) a pair of real solutions

$$\alpha_0^0 = \frac{E_{T_2}}{\gamma_0} \tag{15}$$
$$\alpha_1^0 = \sqrt{\sqrt{\frac{\gamma_2}{\gamma_1}}\frac{E_p - E_{T_2}}{\chi_{12}\left[h_2\,(h_1-h_2+h_{12})^2-(h_1-h_2+h_{12})+h_1\right]}}, \qquad \alpha_2^0 = -\left(\alpha_1^0\right)_{\substack{\gamma_1\leftrightarrow\gamma_2\\ h_1\leftrightarrow h_2}}$$

emerges for $E_p > E_{T_2} > 0$.

ii) For *strong cross-coupling* ($\chi_{12} > 2\sqrt{\chi_1\,\chi_2}$) we have an imaginary pair of solutions

$$\alpha_0^0 = \frac{|E_{T_2}|}{\gamma_0} \tag{16}$$
$$\alpha_1^0 = \pm i\sqrt{\sqrt{\frac{\gamma_2}{\gamma_1}}\frac{E_p - |E_{T_2}|}{\chi_{12}\left|h_2\,(h_1-h_2+h_{12})^2-(h_1-h_2+h_{12})+h_1\right|}}, \alpha_2^0 = -\left(\alpha_1^0\right)_{\substack{\gamma_1\leftrightarrow\gamma_2\\ h_1\leftrightarrow h_2}}$$

for $E_p > |E_{T_2}| > 0$. An overview on the possible solutions for the various parameter regimes is depicted graphically in Fig. 2.

In a more realistic description we have to relax the condition of zero detunings, since the relevant modes with the largest nonlinear coupling strengths are in general not degenerate in frequency. The numerical analysis indicates that for small detunings

the general classification of solutions is still useful as a guideline, and especially in the weak cross-coupling case the dynamical behaviour of the solutions remains similar. For the strong cross-coupling case this behaviour is only found up to a certain critical detuning. Beyond this, no steady state exists any more and one finds oscillatory (time dependent) solutions, as shown and discussed in section 4.

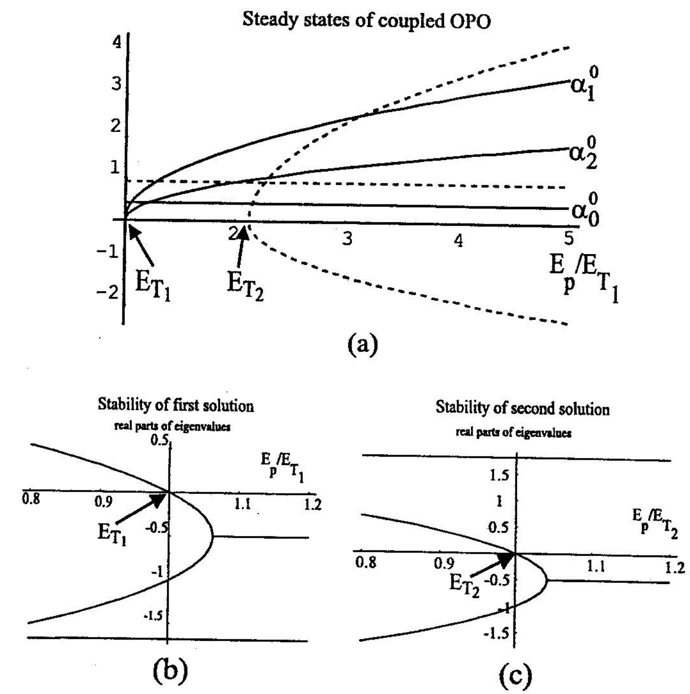

Fig. 3. (a) Steady state solutions as a function of pump strength. (b),(c) Linearized stability analysis.

3.2 Linearized stability analysis

Since mainly the stable solutions are directly observable in practice, we will now discuss the stability of the various solutions in particular operating regimes. This is done by a linear stability analysis for the equations of motion Eq. (10); the negativity of the real parts of the eigenvalues of the Jacobian matrix at the various steady state solutions is checked numerically. Let us again consider the two cases:

(i) weak cross-coupling (mainly degenerate OPO)

Fig. 3a shows the 'same sign' (solid lines) and 'opposite sign' (dashed lines) solutions, which appear above their thresholds. In Fig. 3b we show that all real parts of the eigenvalues of the linearized matrix evaluated at the solutions $\{E_{T_1}/\gamma_0, \pm r_1, \pm r_2\}$ become negative when crossing the threshold from below; this means that this pair of solutions becomes stable above its threshold. Its stability remains furthermore unchanged upon crossing the second threshold E_{T_2}. In contrast to this, Fig. 3c demonstrates that the pair of solutions with opposite signs in α_1 and α_2, i.e. $\{E_{T_2}/\gamma_0, \pm R_1, \mp R_2\}$, remains unstable even above its threshold of existence E_{T_2}. Therefore, in the present case, the pair with the same sign represents the only stable pair above E_{T_1}, at least for the parameters depicted here. Since the functions determining the stability of the various solutions are polynomials of high order, it is impossible to prove that the behaviour depicted in Figs. 3(a-c) is universal in parameter space; however, numerous numerical simulations of the equations of motion have increased our confidence that the remaining parameters, as for instance the damping rates, play no essential role. Nonzero detunings, however, lead to a qualitative change of these results.

(ii) strong cross-coupling (mainly nondegenerate OPO)
As before, the solutions $\{E_{T_1}/\gamma_0, \pm r_1, \pm r_2\}$ become stable above their threshold E_{T_1}. Here the second pair emerging for $E_p > |E_{T_2}|$, namely $\{E_{T_1}/\gamma_0, \pm iR_1, \mp iR_2\}$ turns out to be be purely imaginary. Physically this means that the fields in the modes a_1 and a_2 are generated by nondegenerate downconversion and feedback to the pump via sum-freqency generation. It is interesting to note that above its threshold this second solution is stable against amplitude fluctuations, but unstable against phase noise; in numerical simulations we found that starting close to this solution, the system can remain there for a relatively long time in terms of inverse cavity decay rates, before it suddenly flips its phase and returns to the first solution. For convenience the results on the stability of the various solutions are also summarized in Fig. 2.

3.3 Discussion

Let us now briefly add some comments on the dynamics of this model. Below all threshholds only the pump field oscillates and all other modes contain only noise. However, the intermode coupling could still be observed in the modified spatial photon correlations. In our model a photon in one mode is correlated with either one in the same mode determined by amplitudes proportional to χ_1 and χ_2 or with a photon in the other mode with an amplitude proportional to χ_{12}. If one can spatially separate the two modes, this behaviour should be observable. Also the lowering of the thresholds as a function of the pump size could be investigated.

Above threshold the effect should be even more drastic, as one would get simultaneous fixed phase oscillation of the two modes. In Fig. 4a as an example we have plotted the time evolution of all modes for linearly increasing pump strength. Both modes start to oscillate simultaneously at the predicted lowered threshold and the pump field (short dashed line) is clamped at its threshold value. The signal and idler modes (solid lines) increase with the pump amplitude as expected. We find that this oscillation is stable against small perturbations in amplitude and phase. For different initial conditions also the stationary solution with both signs (α_1 and α_2) reversed appears and is stable (long dashed lines).

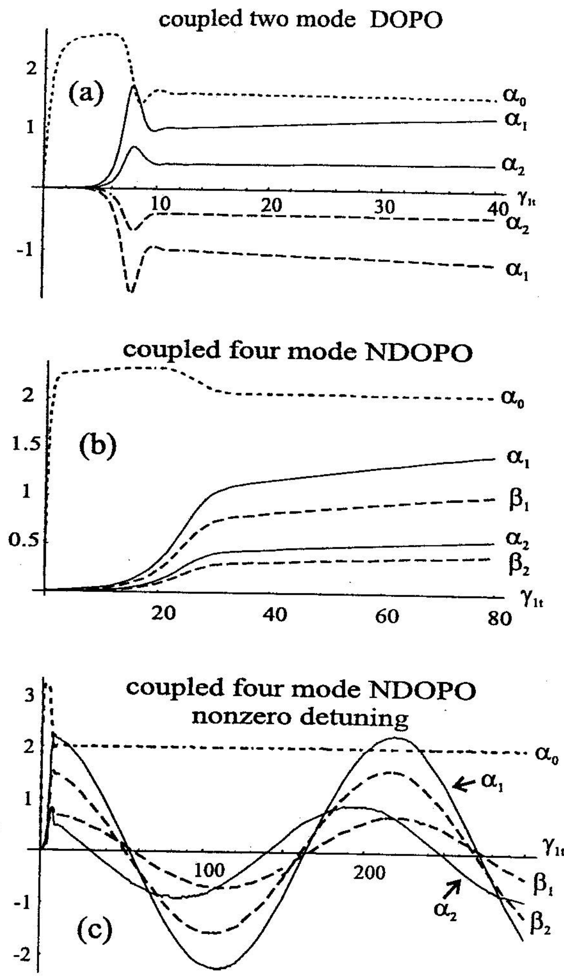

Fig. 4. Dynamics of the multimode OPO.

4. Nondegenerate four and more mode case

As is obvious from Fig. 1, in a more realistic description accounting for finite pump-field size, the restriction to just two modes is somewhat artificial and more signal as well as pump modes (fed by sum frequency generation processes) should be considered. In such a model an analytic solution for steady steades and thresholds seems rather tedious and we retreat mainly to numerics here.

As a first generalisation we look at the case of simultaneous multiple nondegenerate operation (i.e $\omega_i \neq \omega_s$) involving two pairs (α_1, β_1) and (α_2, β_2) which are additionally cross-coupled. Without detunings the system's behaviour is very similar to the previous case, with the main difference stemming from the possibly different decay rates of the various modes involved. Again one finds a modification of the thresholds and multistability between different steady state solutions. We will not give explicit analytical expressions here, but demonstrate the behaviour numerically. The possibility of phase stable combined four-mode-operation is shown in Fig. 4 b. In position space this would manifest itself in the appearence of a stable radial pattern. This situation is quite changed, if one allows some of the modes to be detuned. In this case the combined oscillation leads to an oscillating type of behaviour involving all the modes *except for the pumpfield*, as shown in Fig. 4c; starting from vacuum the systems evolves towards a quasi steady state as above, but then immediately periodic oscillations start. Note that in contrast to selfpulsing the pump field remains constant. Qualitatively new effects can also be obtained in the case with even more modes participating. In the limit of a very large number of contributing modes it is, however, advantageous to leave the mode picture and work in the spatial domain [7].

5. Conclusions

We have shown that considering a cavity geometry where the transverse mode splitting is not very large [e.g. a (quasi-)planar/confocal/spherical cavity] and taking the finite size of the pumpfield (which could e.g. be mode-matched to the same cavity) into account, can dramatically change the behaviour of the triply resonant OPO (TROPO). Intermode coupling leads to simultaneous multimode oscillation as well as spatially modified photon statistics. This is of course related to the occurrence of optical patterns in the many mode limit.

Acknowledgements This work was supported by the TMR-Network *Quantum Structures* and the Fonds zur Förderung der wissenschaftlichen Forschung (Projekt S6506). M.M. acknowledges support via the *APART* fellowship of the Österreichische Akademie der Wissenschaften.

References

[1] Special issue on Second Order Nonliner Optics: *J. Opt. Soc. Am. B* **9** (1997) 2
[2] see e.g. G.L. Oppo, M. Brambilla, L.A. Lugiato: *Phys. Rev. A* **49** (1994) 2028
[3] I. Marzoli, A. Gatti, G. Lugiato: *Phys. Rev. Lett.* (1997) in print
[4] Siegman: *Lasers* (Unversity Science books, Mill Valley, CA, 1986)
[5] A. Yariv: *Quantum Electronics*, 3rd ed. (Wiley, New York, 1989)
[6] C. Fabre et al.: to be published
[7] A. Gatti, H. Wiedemann, L.A. Lugiato, I. Marzoli, G.L. Oppo, S.M. Barnett: *Phys. Rev. A* (1997) to be published